Electronic Supplementary Material (ESI) for ChemComm.

Supporting information

A 3D Free-standing Lithiophilic Silver Nanowire Aerogel for Lithium Metal Batteries without Lithium Dendrite and Volume Expansion: *In Operando* X-ray Diffraction

Nutthaphon Phattharasupakun,[a,b] Juthaporn Wutthiprom, [a,b] Salatan Duangdangchote[a,b] and Montree Sawangphruk[a,b,]*

[a]Department of Chemical and Biomolecular Engineering, School of Energy Science and Engineering, Vidyasirimedhi Institute of Science and Technology, Rayong 21210, Thailand

[b]Centre of Excellence for Energy Storage Technology (CEST), Vidyasirimedhi Institute of Science and Technology, Rayong 21210, Thailand

Section 1: Experimental section

Synthesis of 3D AgNWA. The 3D AgNWA was synthesized by a modified polyol reduction method.[1] Briefly, 3.84 g PVP (Polyvinylpyrrolidone, MW~1,300,000, Sigma Aldrich) was firstly dispersed in 233 ml EG (99.5% Ethylene glycol, QRec). Then, 5.28 ml of 0.01 M NaCl (99.5% Sodium chloride, Carlo erba) in EG and 1.94 ml of 0.01 M of $Fe(NO_3)_3 \cdot 9H_2O$ (98% Ferric nitrate, Univar) in EG was added into the PVP solution which will be labelled as a stock solution A. For stock solution B, 3.852 g $AgNO_3$ (Panreac Applichem) was dispersed in 240 ml EG. After that, 400 ml EG solution was separately heated to 170 ˚C. The stock solution A and B were simultaneously dropped into the EG solution while kept stirring. The EG solution was further heated for 15 min after the addition of solution A and B. After that, the solution was kept stirring until reached room temperature in which the obtained products contain both Ag nanowires and Ag nanospheres. The AgNWA were separated by washing with acetone and re-dispersed in DI water several times. For 3D AgNWA free-standing electrode, the AgNWA product was dispersed in DI water, frozen with liquid N_2, and finally freeze-dried for 72 h. The synthesis procedure can be seen in the schematic diagram in Fig. S1.

Morphological and structural characterizations. The morphology of the AgNWA and electrodes was characterized by Field-emission scanning electron microscopy (FESEM, JSM-7001F, JEOL Ltd.) and Transmission electron microscopy (TEM, JEM-ARM200F, JEOL Ltd.). The crystallographic structure of the samples was investigated by X-ray diffraction (XRD, Bruker, D8 Advance) using a Cu Kα radiation (λ = 1.54056 Å). For *ex situ* measurement, the electrode was dissembled using a hydraulic disassembling machine and then washed with DME (99.5% 1,2-Dimethoxyethane, Sigma-Aldrich) to remove Li salts. It was naturally dried inside a glove box. The dried electrode was transferred to an air-sensitive holder for FESEM measurement without air exposing. For *in operando* XRD, the measurement was set up in an XRD cell (LRCS, Amiens) coupling with D8 Advance XRD machine. The Rietveld refinement analysis was carried out using TOPAS software version 5.0 (Bruker AXS). The $LiFePO_4$ and $FEPO_4$ in an orthorhombic structure with space group Pnma were used in a two-phase Rietveld refinement. The first scan of *in situ* data was initially refined using Chebychev polynomial third order background with a calculation step

of 0.02 in the 2Theta of 15-38^{o} excluding the Bragg reflections from Al and Be window (Fig. S21). Then, the sequential refinements for all in situ datasets were performed.

Electrochemical evaluation of electrodes. The AgNWA free-standing electrode was prepared by rolling the as-obtained AgNWA after freeze-drying method. The electrode was then punched into a circular shape with an area of 1 cm^2. The 3D AgNWA electrode was used as a working electrode and fabricated with metallic lithium as a counter electrode in a coin-cell 2025 in an argon-filled glove box with oxygen and water less than 1 ppm (Mbraun labstar glove box workstation). A planar copper foil was also used for a control experiment. Polyethylene film (thickness~25 μm) was used as a separator and a controlled amount of 80 μl of 1.0 M $LiPF_6$ (98% Lithium hexafluorophosphate) in 1:1 v/v of EC (98% Ethylene carbonate, Aldrich)/DEC (99% Diethyl carbonate, Aldrich) was used as an electrolyte. For Li deposition, the electrodes were discharged to a fixed Li plating capacity of 1 mAh cm^{-2} and then charged back to 1.0 V at different applied areal currents of 0.5, 1.0, and 2.0 mA cm^{-2}. All the electrochemical performances were tested using a NEWARE battery tester. In case of the Li-AgNWA electrode for symmetric cell and full cell, the 3D AgNWA electrode was firstly lithiated with 10 mAh cm^{-2} of Li at 0.5 mA cm^{-2}. After that the cell was disassembled for which the electrode was further used to fabricate a symmetric cell or full cell. For the LFP electrode, the LFP powder (Gelon, Hongkong) was mixed with conductive carbon black (TIMCAL) and PVDF binder (Poly(vinylidene fluoride), Mw ~534,000, Sigma-Aldrich) in a weight ratio of 8:1:1 in NMP (99.5% 1-Methyl-2-Pyrrolidone, QRec). The homogeneous slurry was casted on carbon paper substrate and then cut into an area of 1 cm^2 (SGL Carbon SE, Germany) and finally dried at 80 ˚C for 24 h. The active mass loading (LFP) of each electrode is *ca.* 2.5 mg cm^{-2}. For *in operando* XRD measurement, the LFP slurry was casted on aluminium foil (a thickness of 16 μm) and used as the working electrode for X-ray transparency. For GITT measurement, the diffusion coefficient of Li ions was calculated using the Fick's second law of diffusion as shown in equation (S1 and S2):

$$D = \frac{4}{\pi\tau}\left(\frac{m_B V_m}{M_B S}\right)^2\left(\frac{\Delta E_s}{\Delta E_t}\right)^2 \quad \text{(S1)}$$

$$D = \frac{4L^2}{\pi\tau}\left(\frac{\Delta E_s}{\Delta E_t}\right)^2 \quad \text{(S2)}$$

where D is the chemical diffusion coefficient, τ is the constant current pulse of time, $m_B V_m/M_B$ is the volume of electrode material, L is the thickness of electrode, S is the area of electrode, E_s is the open circuit potential during a single-step GITT, and E_t is the potential during a constant current pulse τ of a single-step GITT. The pulse current at 0.5C was applied for 5 min with a relaxation time of 1h.

Calculation of surface diffusion barrier energy. The surface diffusion barrier energy was investigated using density functional theory (DFT) via using a Vienna *ab initio* simulation package (VASP).[2-4] The interaction between ion cores and valence electrons was accounted by the projector-augmented wave (PAW) pseudopotentials.[5] The exchange and correlation interactions between electrons was treated within the generalized gradient approximation (GGA)[6] with the Perdev-Burke-Ernzerhof (PBE)[7] parameterization. A plane-wave basis was set with a cut-off energy of 400 eV. The convergence thresholds for geometry optimizations were set at 10^{-5} eV and 0.005 eV $Å^{-1}$ for each electronic step and ionic step, respectively. A vacuum region ($_{vac}$d) at least 20 A˚ thickness was used to separate the surface to avoid periodic interactions along a *c*-axis. The diffusion pathway was obtained by comparing the binding energies of the lithium adatom at the high symmetry points along the surface, letting the adatom relax in the direction parallel to the slab. The intermediate calculations are obtained by connecting the two binding sites. The 3×3 supercells were used to minimize the interactions between periodic images of adatoms.

Section 2: Calculation detail of Li accommodation capability in the AgNWA electrode

The Li accommodation capability in the AgNWA electrode can be calculated as follows:[8]

Volumetric capacity of Li = Theoretical specific capacity of Li × Density of Li

$= 3860 \text{ mAh g}^{-1} \text{ x } 0.534 \text{ g cm}^{-3}$

$= 2061.24 \text{ mAh cm}^{-3}$

Plated capacity of Li in AgNWA electrode is *ca.* 70 mAh

Surface area of current collector = 1 cm^2

Volume of plated Li = Plated capacity of Li / Volumetric capacity of Li

$= 70 \text{ mAh} / 2061.24 \text{ mAh cm}^{-3}$

$= 0.034 \text{ cm}^3$

Areal weight of Li = Density of Li × Volume of plated Li / Surface area of current collector

$= 0.534 \text{ g cm}^{-3} \text{ x } 0.034 \text{ cm}^3 / 1 \text{ cm}^{-2}$

$= 18.16 \text{ mg cm}^{-2}$

Areal capacity of Li = Plated capacity of Li / Surface area of current collector

$= 70 \text{ mAh x } 1 \text{ cm}^{-2}$

$= 70 \text{ mAh cm}^{-2}$

Section 3: Additional results

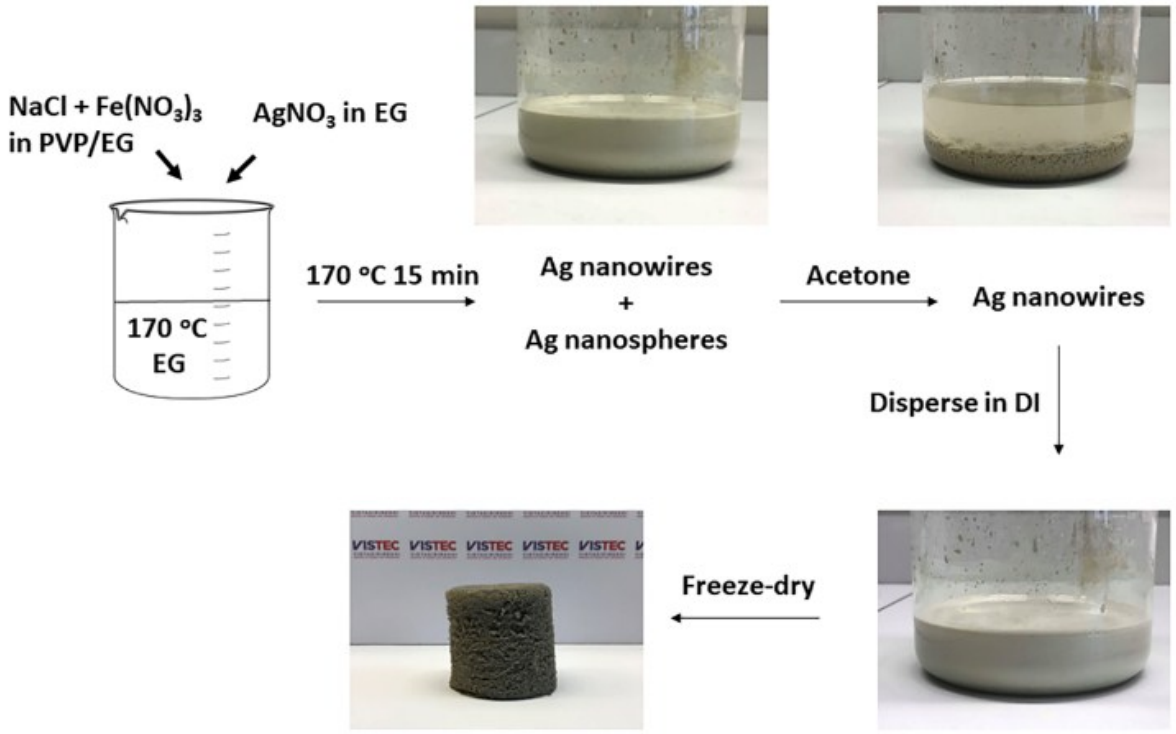

Fig. S1. A schematic showing the synthesis process of 3D AgNWA.

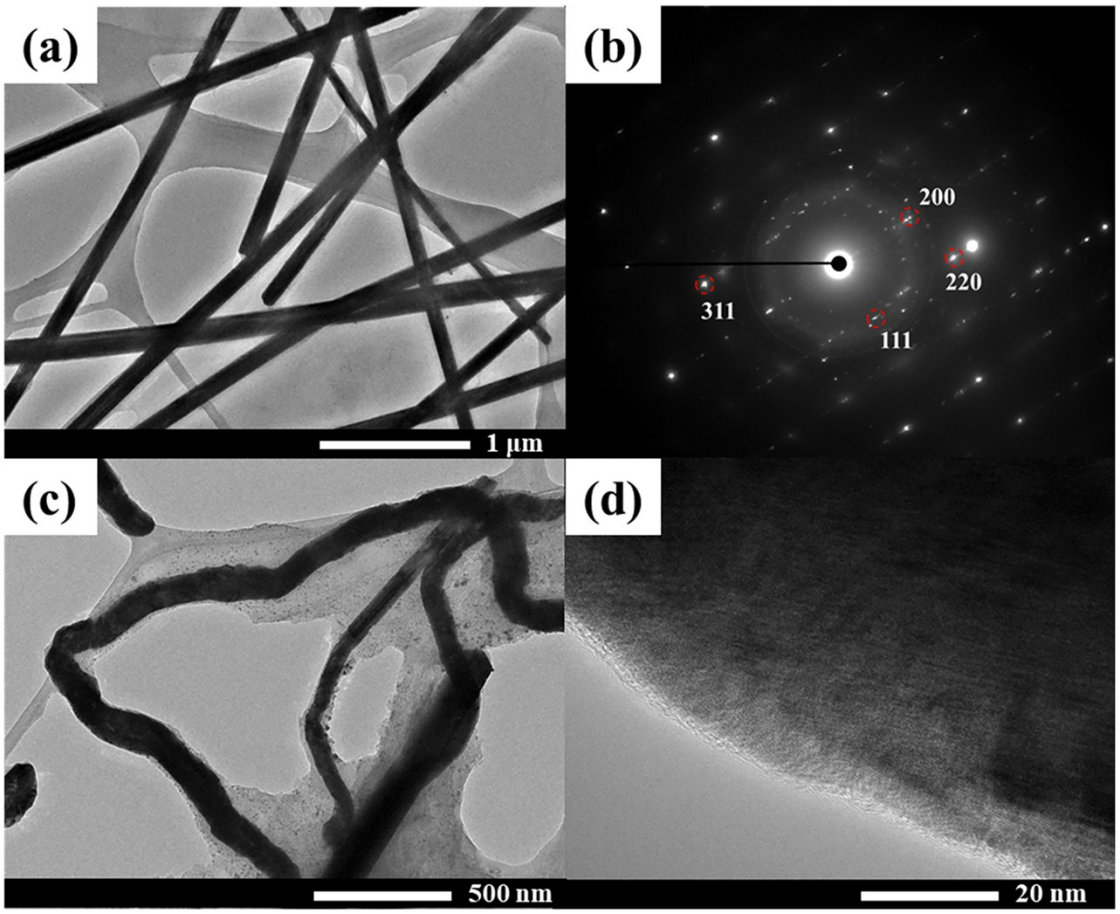

Fig. S2. (a) TEM image and (b) SAED pattern of 3D AgNWA and (c-d) *Ex situ* TEM images of Li-AgNWA with different magnifications after Li plating at 0.5 mA cm^{-2} and 1.0 mAh cm^{-2}.

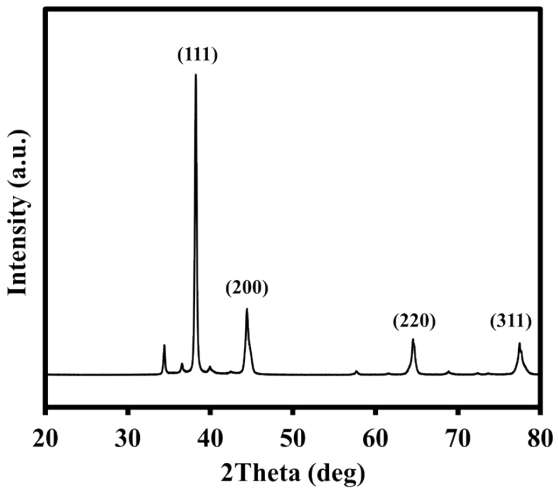

Fig. S3 XRD pattern of AgNWA.

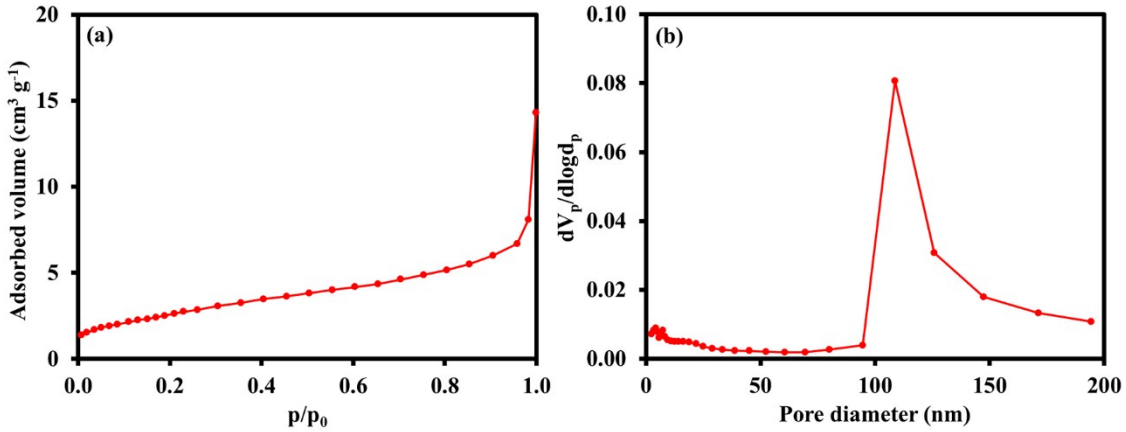

Fig. S4 (a) N_2 adsorption isotherm and (b) BJH pore size distribution of AgNWA.

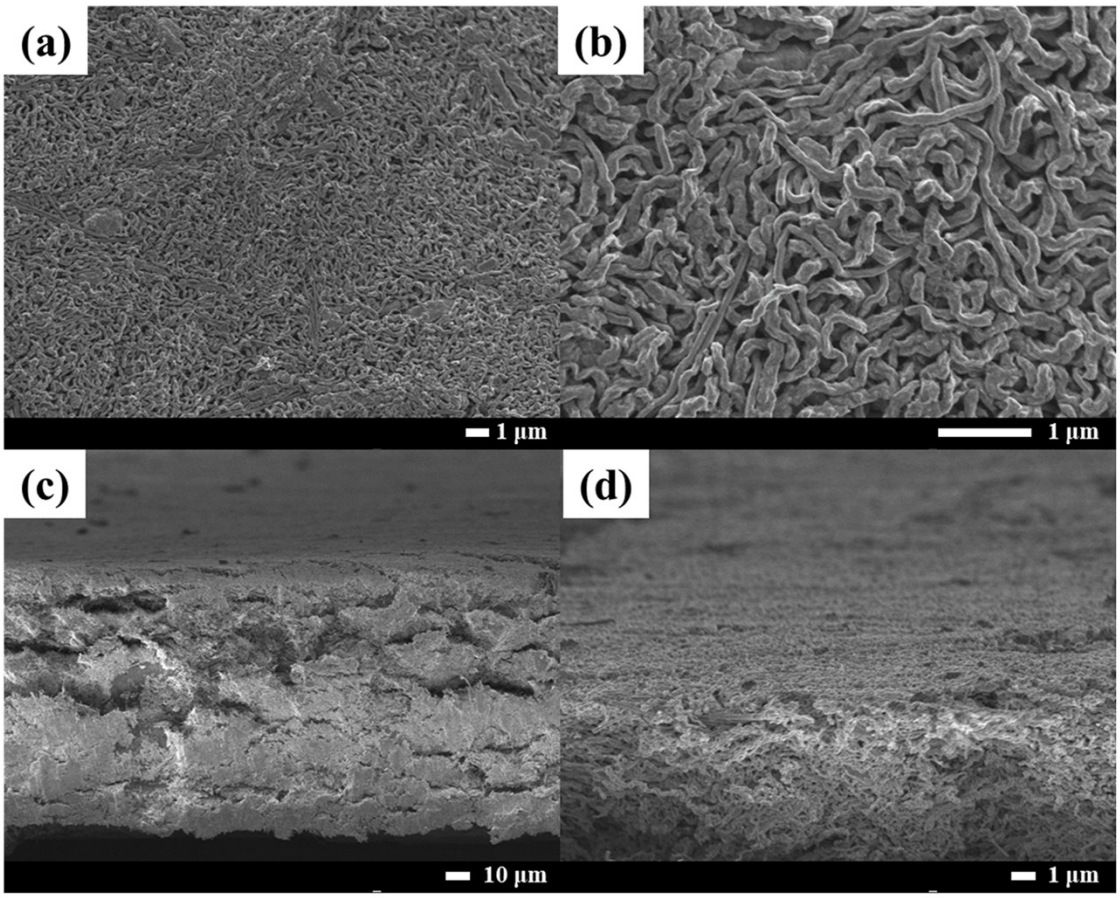

Fig. S5 Low-magnification FESEM images of AgNWA electrodes at (a-b) top-view and (c-d) cross-sectional-view after lithium plating-stripping for 20 cycles.

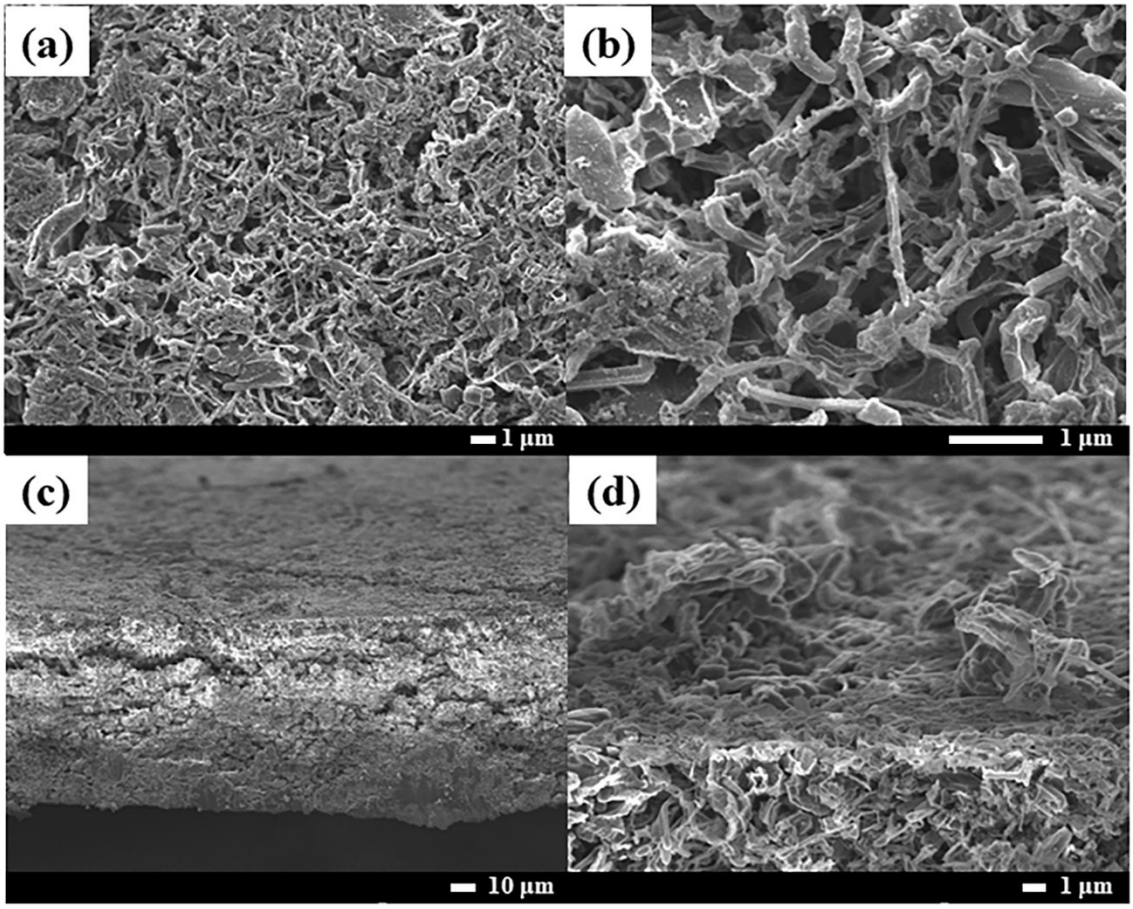

Fig. S6 FESEM images of planar Cu electrodes at (a-b) top-view and (c-d) cross-sectional-view after lithium plating-stripping at 1.0 mA cm^{-2} and 1.0 mAh cm^{-2} for 20 cycles.

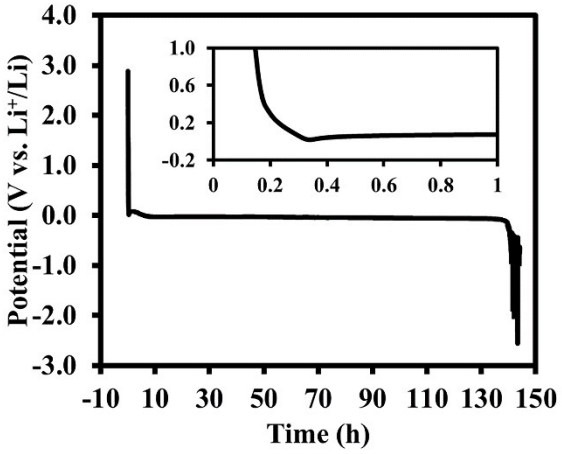

Fig. S7 Discharge profile of a unidirectional galvanostatic Li plating on AgNWA at 0.5 mAcm^{-2}.

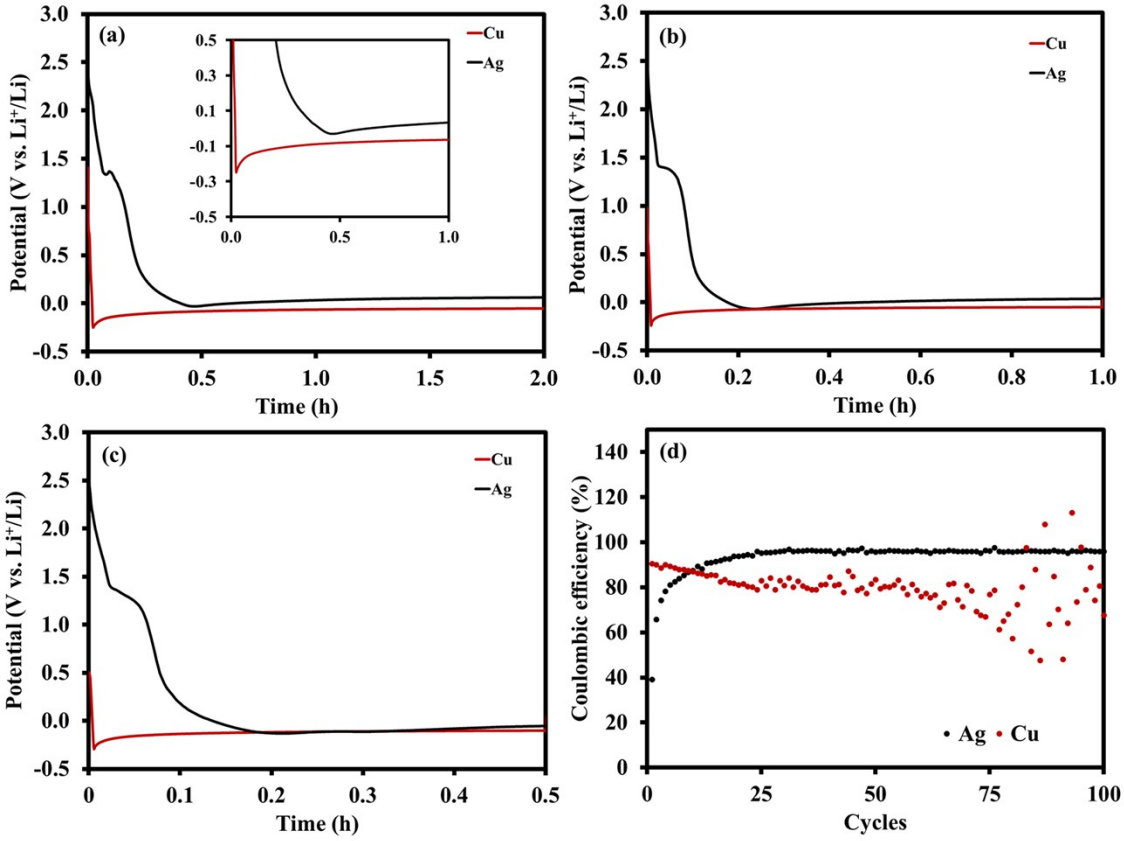

Fig. S8 GCD profiles of AgNWA//Li and Cu//Li batteries at the first discharge process at different current densities of (a) 0.5, (b) 1.0, and (c) 2.0 mA cm^{-2} and (d) coulombic efficiency at 0.5 mA cm^{-2} and 1.0 mAh cm^{-2}.

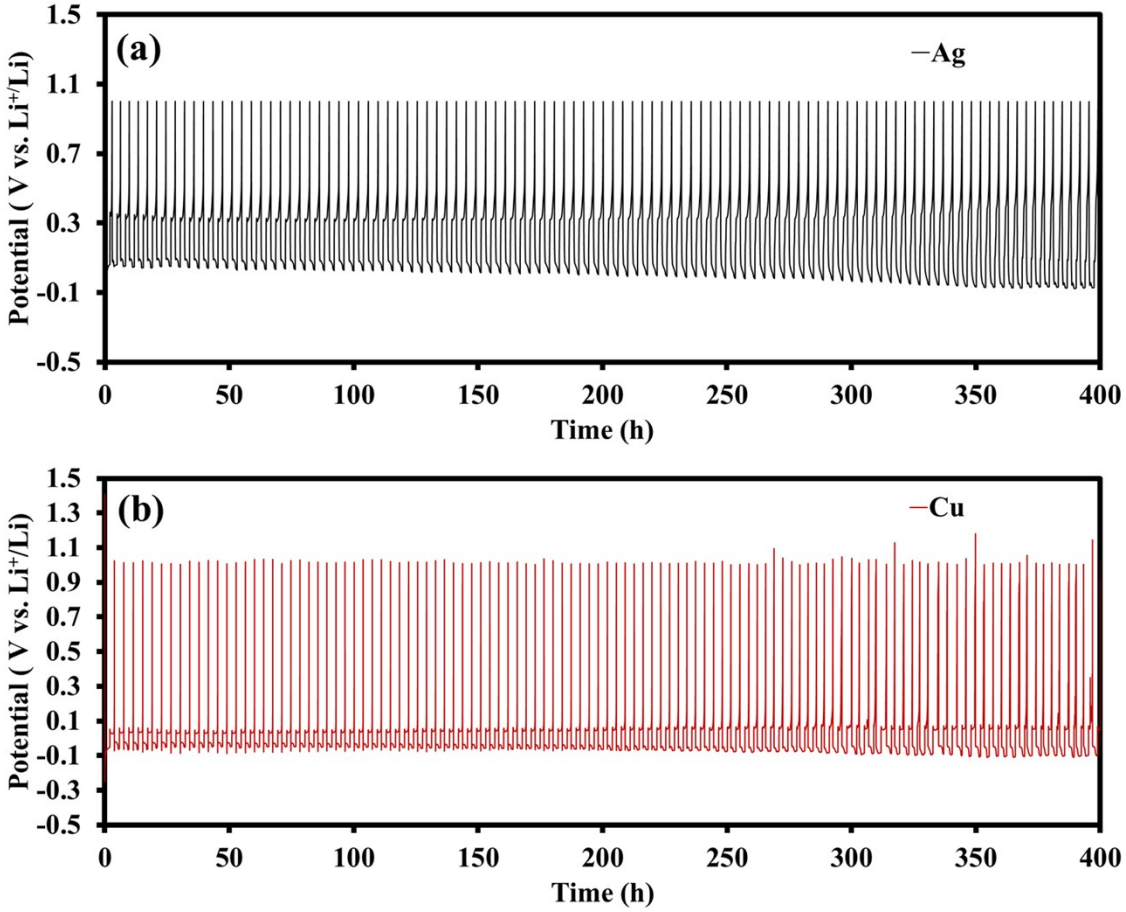

Fig. S9 GCD profiles at 0.5 mA cm^{-2} and 1.0 mAh cm^{-2} of (a) AgNWA//Li and (b) Cu//Li batteries.

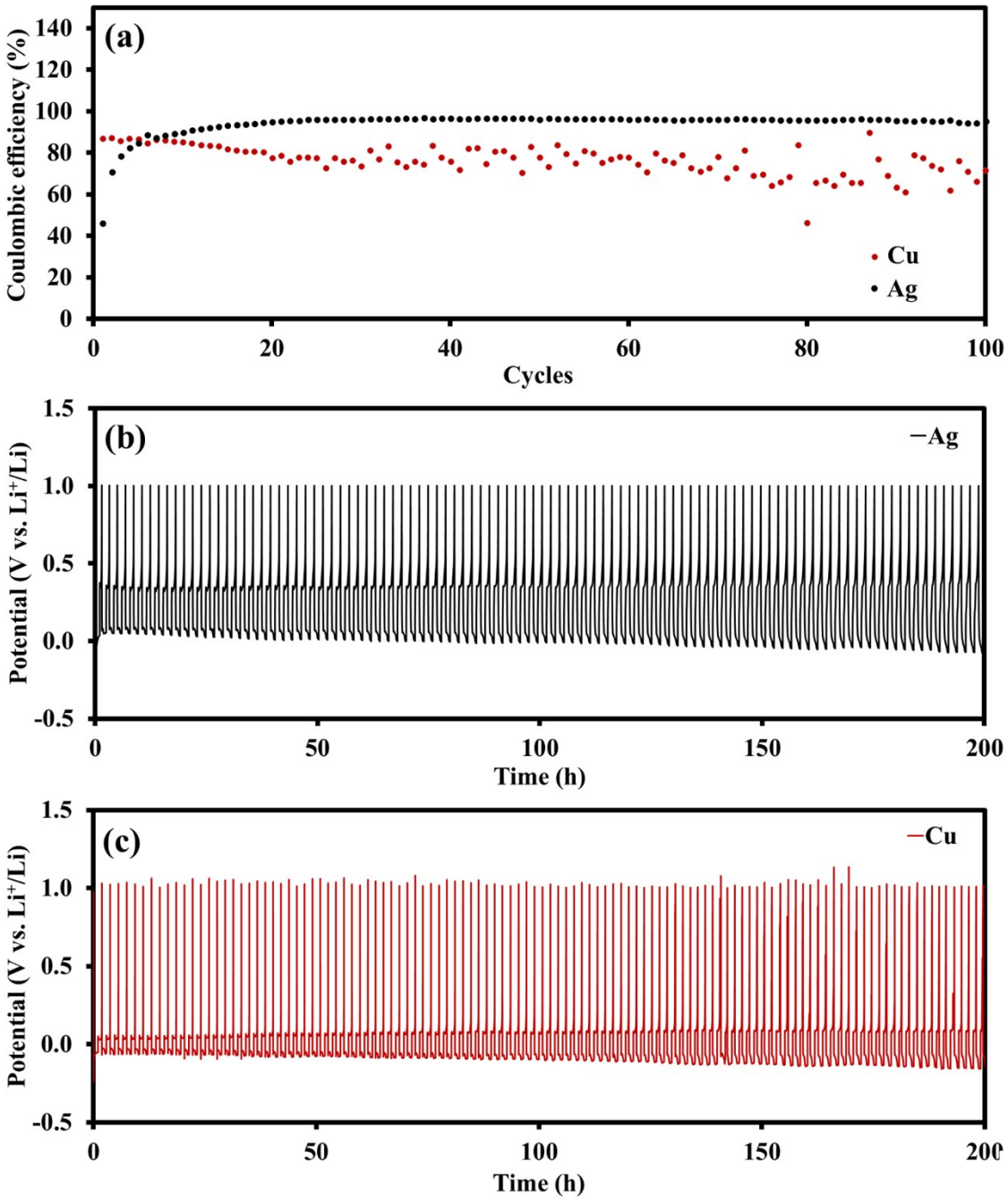

Fig. S10 Stability test of AgNWA//Li and Cu//Li batteries including (a) Coulombic efficiency and (b-c) GCD profiles at 1.0 mA cm^{-2} and 1.0 mAh cm^{-2}.

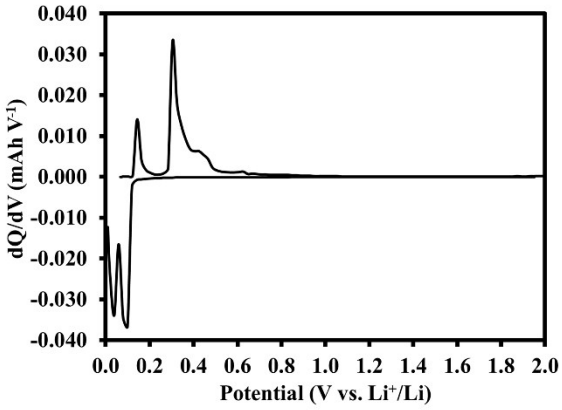

Fig. S11 Differential capacity curve of lithiation on AgNWA.

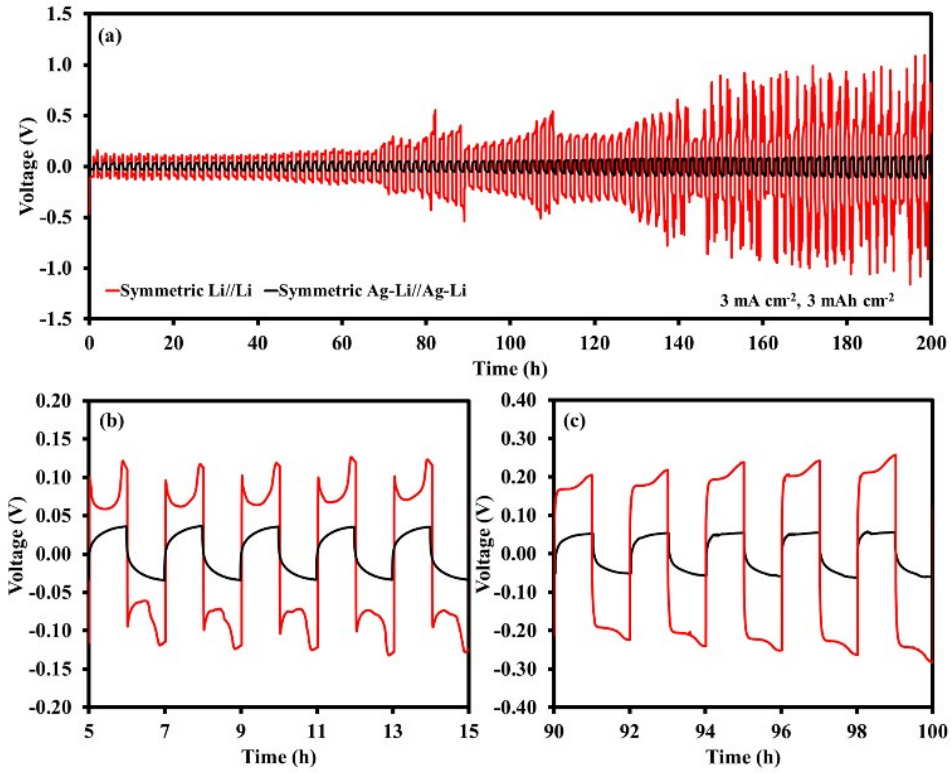

Fig. S12 Charge-discharge profiles of symmetric Li//Li and Li-AgNWA//Li-AgNWA cells at a current density of 3 mA cm^{-2} (3 mAh cm^{-2}).

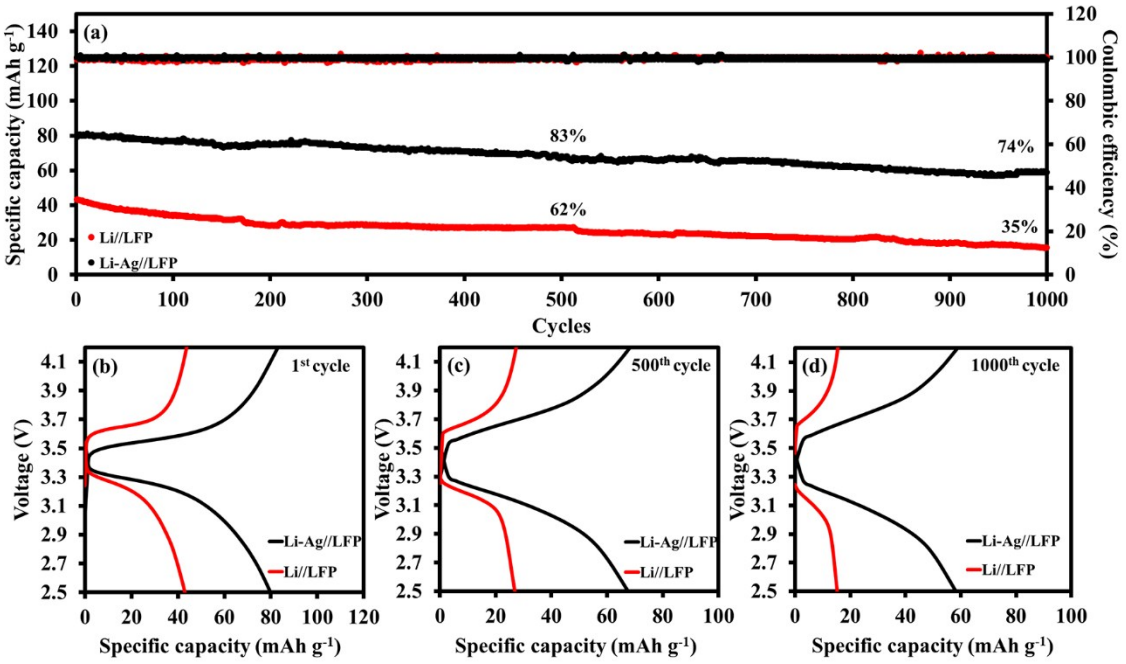

Fig. S13. (a) Cycling stability up to 1000 cycles at 5.0 C and charge-discharge profiles at (b) 1st, (c) 500th, and (d) 1000th cycle of Li//LFP and Li-AgNWA//LFP full-cells with LFP active mass loading of 5 mg cm^{-2}.

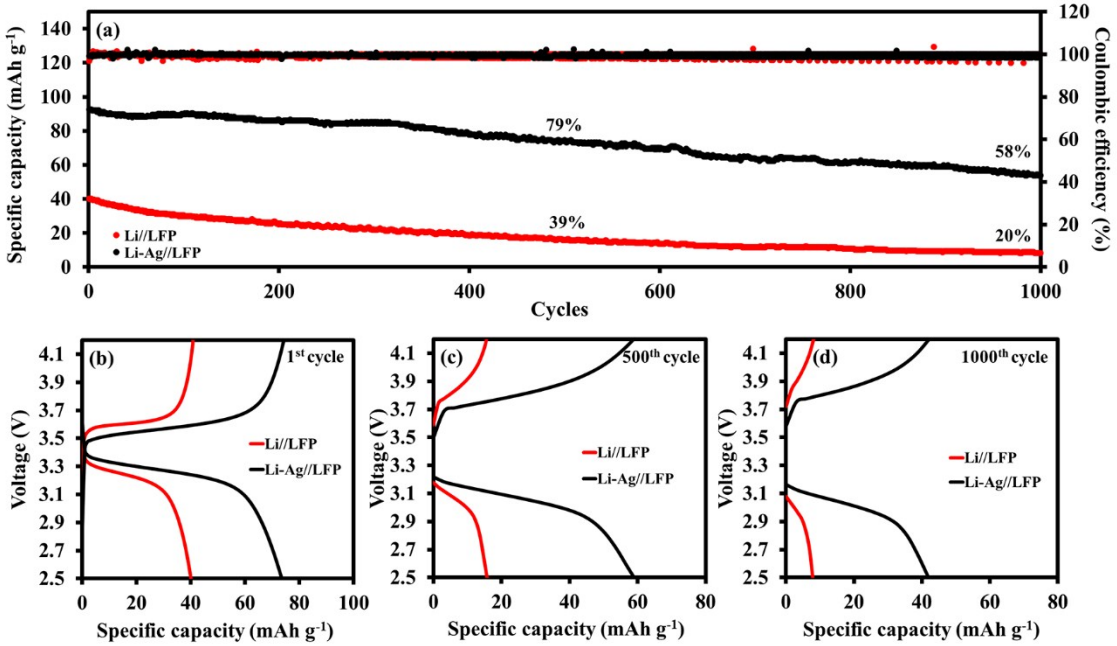

Fig. S14. (a) Cycling stability up to 1000 cycles at 5.0 C and charge-discharge profiles at (b) 1st, (c) 500th, and (d) 1000th cycle of Li//LFP and Li-AgNWA//LFP full-cells with LFP active mass loading of 10 mg cm^{-2}.

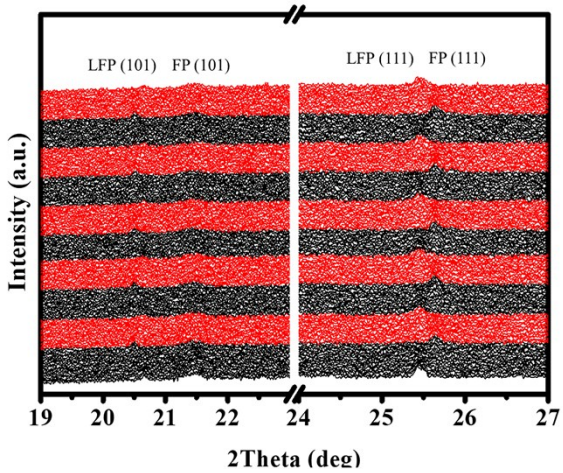

Fig. S15 *In operando* XRD spectra of Li-AgNWA//LFP cell tested at 0.5C for 5 cycles.

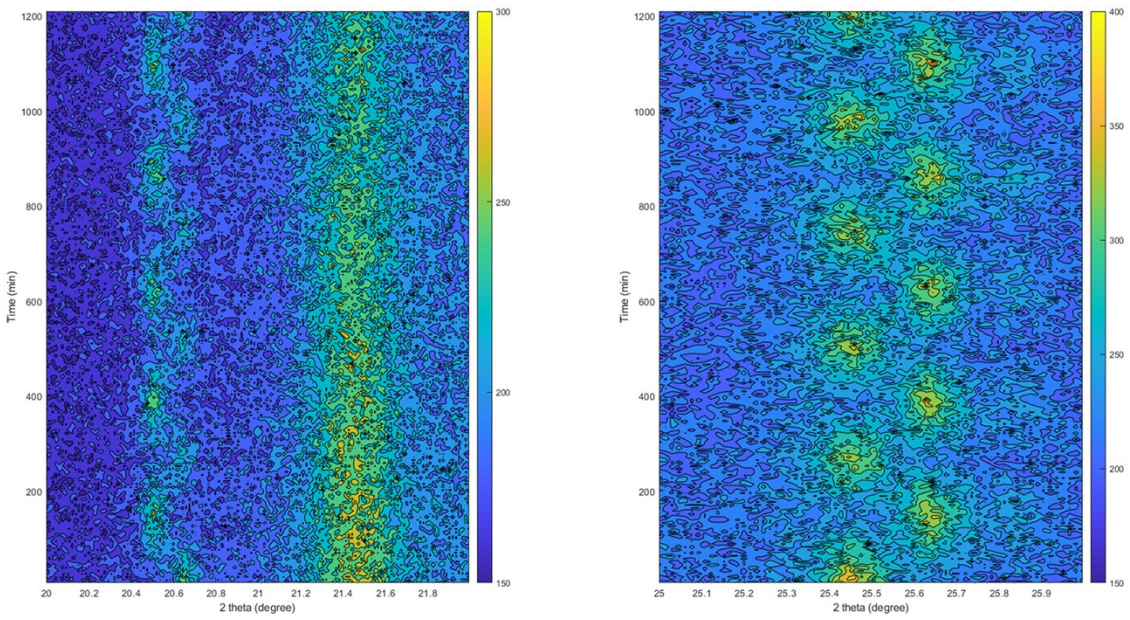

Fig. S16 2D plots of *in operando* XRD results of Li-AgNWA//LFP cell tested at 0.5C for 5 cycles.

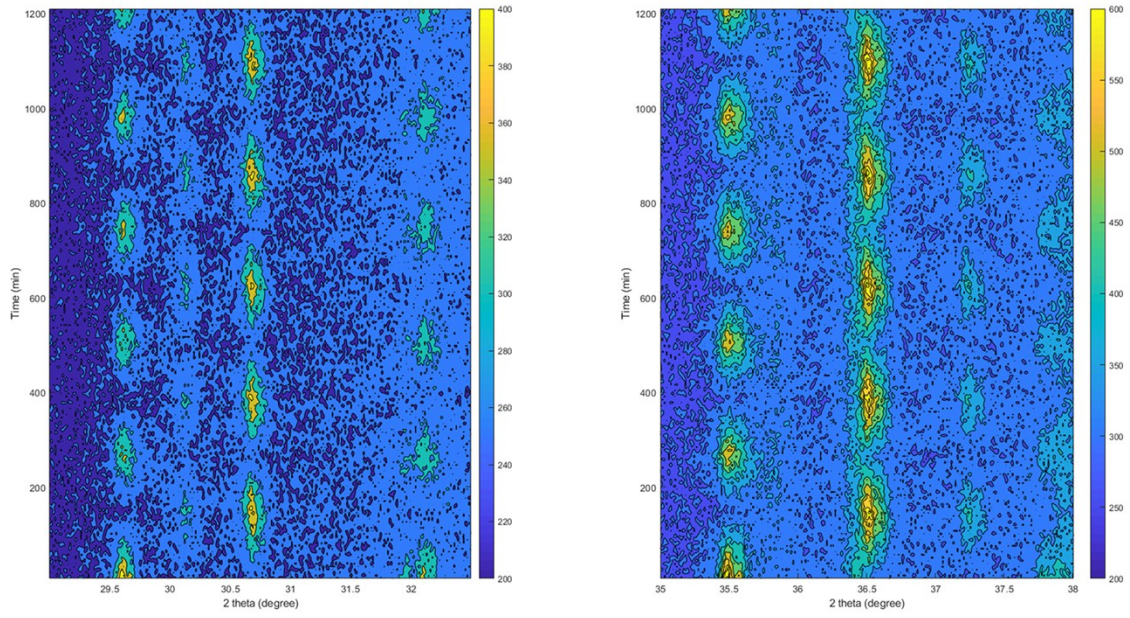

Fig. S17 2D plots of *in operando* XRD results of Li-AgNWA//LFP cell tested at 0.5C for 5 cycles.

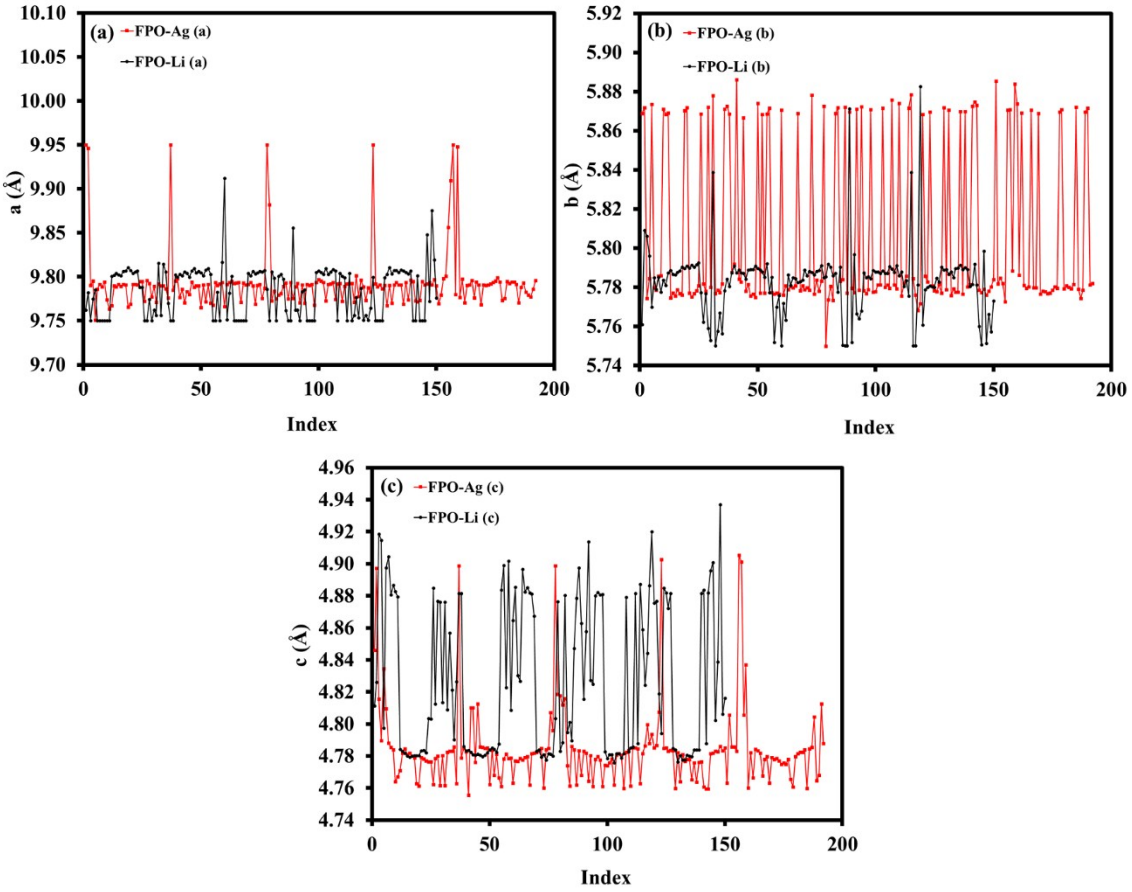

Fig. S18 Lattice parameter (b) a, (c) b, and (d) c changes of FPO during charging/discharging processes of Li-AgNWA//LFP cell compared with Li//LFP cell.

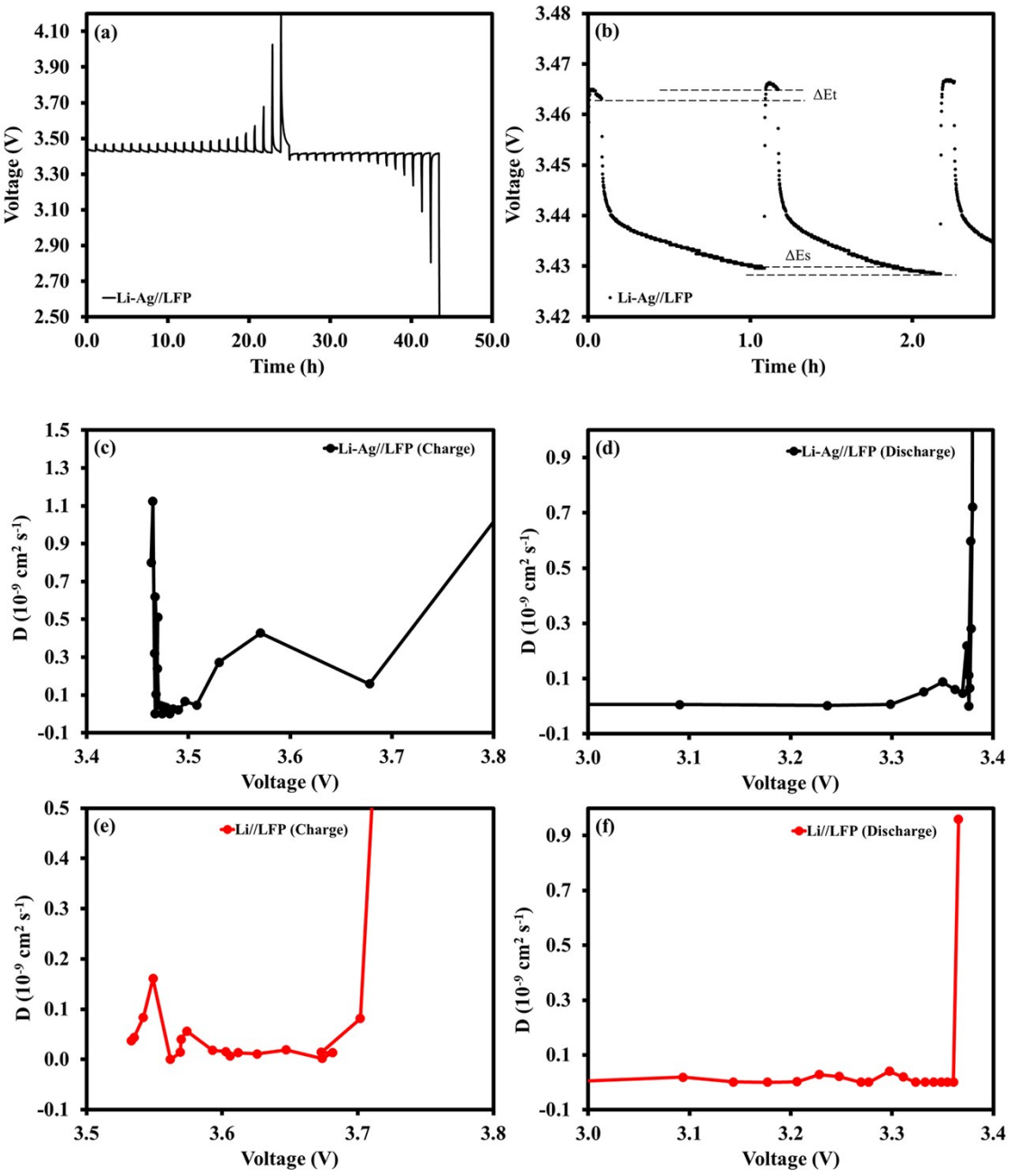

Fig. S19 (a) GITT charge/discharge profiles, (b) Potential profile at a constant current pulse and relaxation, and diffusion coefficient of Li ions in (c-d) Li-AgNWA//LFP and (e-f) Li//LFP during charging and discharging.

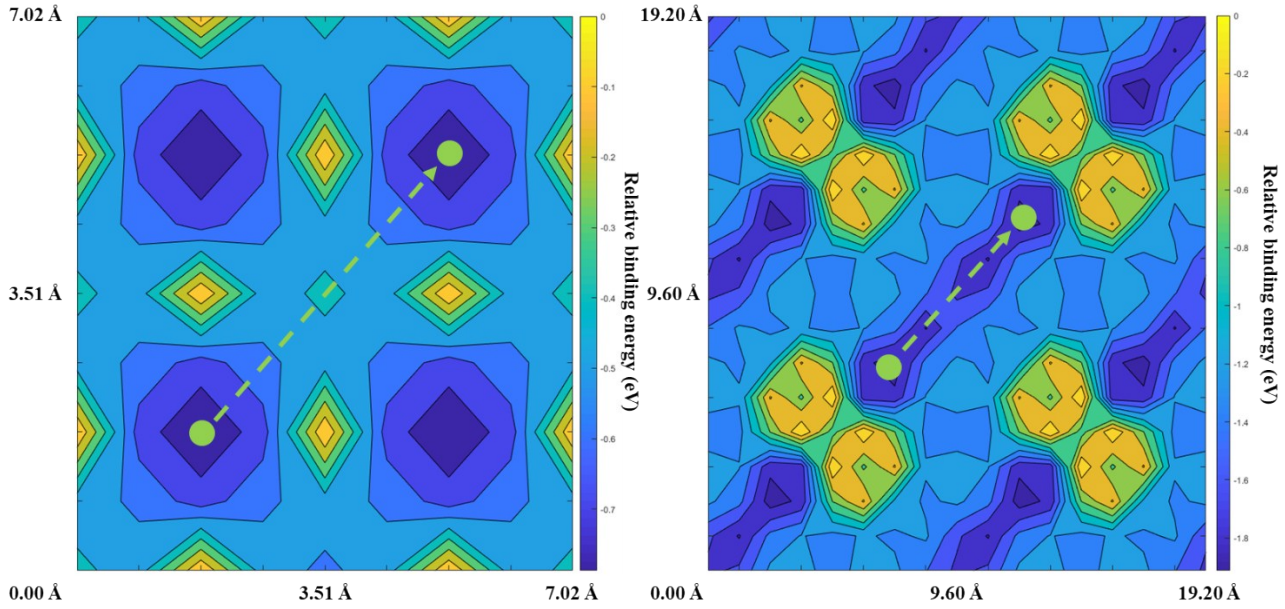

Fig. S20 Surface binding energies versus the cell coordinate of (a) body-centered cubic lithium structure, and (b) lithium-silver structure. The lowest energy sites are indicated with a green circle and the diffusion path is shown with the green arrows.

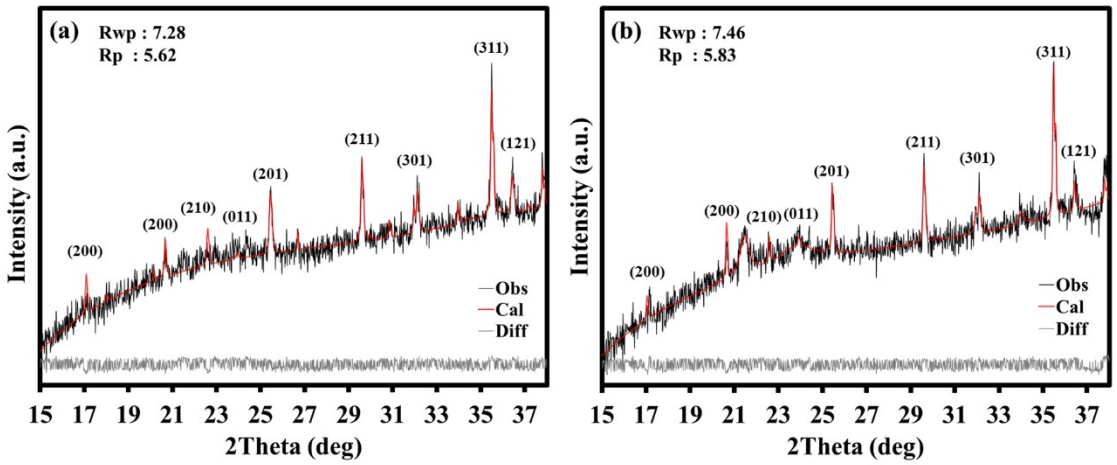

Fig. S21. Rietveld refinement of the first *in situ* XRD pattern of LFP in (a) Li/LFP and (b) Li-AgNWA/LFP cells.

References

1. B. Wiley, Y. Sun and Y. Xia, *Langmuir*, 2005, **21**, 8077-8080.
2. G. Kresse and J. Hafner, *Physical Review B*, 1993, **47**, 558-561.
3. G. Kresse and J. Furthmüller, *Computational Materials Science*, 1996, **6**, 15-50.
4. G. Kresse and J. Furthmüller, *Physical Review B*, 1996, **54**, 11169-11186.
5. G. Kresse and D. Joubert, *Physical Review B*, 1999, **59**, 1758-1775.
6. J. P. Perdew, K. Burke and M. Ernzerhof, *Physical Review Letters*, 1996, **77**, 3865-3868.
7. J. P. Perdew, M. Ernzerhof and K. Burke, *The Journal of Chemical Physics*, 1996, **105**, 9982-9985.
8. C. Jin, O. Sheng, J. Luo, H. Yuan, C. Fang, W. Zhang, H. Huang, Y. Gan, Y. Xia, C. Liang, J. Zhang and X. Tao, *Nano Energy*, 2017, **37**, 177-186.